Phys. Med. Biol. **45** (2000) 3143–3158. Printed in the UK PII: S0031-9155(00)11868-8

Brain perfusion monitoring with frequency-domain and continuous-wave near-infrared spectroscopy: a cross-correlation study in newborn piglets

G Zhang†, A Katz†, R R Alfano†¶, A D Kofinas‡, D A Kofinas‡, P G Stubblefield§, W Rosenfeld‖, D Beyer‡, D Maulik‖ and M R Stankovic‡§‖

† Institute for Ultrafast Spectroscopy and Lasers and New York State Center for Advanced Technology for Ultrafast Photonic Materials and Applications Department of Electrical Engineering and Physics, The City College of the City University of New York, 138th Street and Convent Avenue, New York, NY 10031, USA
‡ Departments of Obstetrics and Gynecology and Medicine, The Brooklyn Hospital Center, The Affiliate of Weill Medical College of Cornell University, 121 De Kalb Avenue, Brooklyn, NY 11201, USA
§ Department of Obstetrics and Gynecology, Boston University School of Medicine, 1 Boston Medical Center Place, Boston MA 02118, USA
‖ Departments of Obstetrics and Gynecology and Pediatrics, Winthrop University Hospital, State University of New York at Stony Brook, 251 First Street, Mineola, New York 11501, USA

Received 14 February 2000, in final form 13 June 2000

Abstract. The newborn piglet brain model was used to correlate continuous-wave (CW) and frequency-domain (FD) near-infrared spectroscopy. Six ventilated and instrumented newborn piglets were subjected to a series of manipulations in blood oxygenation with the effects on brain perfusion known to be associated with brain hypoxia–ischaemia. An excellent agreement between the CW and FD was demonstrated. This agreement improved when the scattering properties (determined by the FD device) were employed to calculate the differential pathlength factor, an important step in CW data processing.

1. Introduction

Numerous studies in humans and animals have demonstrated the importance of disturbances in cerebral haemodynamics and oxygenation in the pathogenesis of perinatal 'hypoxic-haemodynamic' brain injury leading to cerebral palsy, mental retardation and seizures (Meek *et al* 1998, Nelson and Ellenberg 1986, Volpe 1989, Perlman *et al* 1984). Monitoring of these disturbances at the bedside would be the first step in the prevention and treatment of brain injury (Tsuji *et al* 1998). Unfortunately, none of the available techniques can be used to provide this important information. Optical spectroscopy has shown the potential to provide continuous monitoring of brain perfusion and oxygenation in real-time at the bedside (van Houten *et al* 1996, Brun *et al* 1997, Tsuji *et al* 1998, Stankovic *et al* 1998c, Kurth *et al* 1993, Fantini *et al* 1999, Wyatt 1997, Chance *et al* 1997, Hirtz 1993).

Optical spectroscopy uses near-infrared light to non-invasively monitor brain concentrations of oxyhaemoglobin and deoxyhaemoglobin (Alfano *et al* 1997, Wyatt 1997,

¶ Author to whom correspondence should be addressed.

0031-9155/00/113143+16$30.00

Wahr *et al* 1996). For the purposes of optical spectroscopy, haemoglobin is a contrast agent. Therefore, any change in its concentration is detected in optical spectroscopy as a change in tissue perfusion and oxygenation.

Although the majority of the available optical instruments have been tested in phantoms, animals and humans, and validated with the available diagnostic techniques (Stankovic *et al* 1998b, Tsuji *et al* 1998, Wyatt 1997, Wahr *et al* 1996), the question still exists whether or not, and under what conditions, data obtained by different optical instruments would be comparable.

The purpose of this study was to investigate whether or not cerebrovascular changes recorded *in vivo* by continuous-wave (CW) methods would be comparable to those recorded by frequency domain (FD) methods. We hypothesized that the CW spectrometer at City College of New York would be sufficiently sensitive to detect both small and large changes in brain haemodynamics and oxygenation, and that its sensitivity would be comparable to that of the FD instrument at the University of Illinois-ISS, Urbana-Champaign.

2. Material and methods

2.1. Optical spectroscopy

In tissue, light is both absorbed and scattered (Fantini *et al* 1999, Benaron *et al* 1997). Light attenuation is due to: absorption from chromophores of fixed concentration, absorption from chromophores of variable concentration and light scattering (Delpy and Cope 1997). In the absence of scattering, the total light absorption in the medium is a linear sum of that due to each chromophore (Delpy and Cope 1997). In a scattering medium like tissue, this linear summation is distorted because the optical path length at each wavelength may be different (Delpy and Cope 1997). This distorted spectrum is then superimposed upon further wavelength-dependent attenuation arising from light loss due to scatter, which is a complex function of the μ_a and μ_s, scattering phase functions, and tissue and measurement geometry (Delpy and Cope 1997).

Three basic types of optical instruments have been used for the purpose of physiological studies: continuous wave (CW) (Stankovic *et al* 1998b, Tsuji *et al* 1998, Fantini *et al* 1999), time-domain (Alfano *et al* 1998, Benaron *et al* 1997, Delpy *et al* 1988) and frequency-domain (FD) (Fantini *et al* 1999). Unable to determine tissue optical properties, continuous wave instruments cannot provide absolute concentration measurements except for changes from a baseline with no information about whether the baseline value was normal, high or low (Delpy *et al* 1988, Brazy 1991, Wahr *et al* 1996, Delpy and Cope 1997, Fantini *et al* 1999). Time-domain instruments provide scattering information from the mean transit time of picosecond light pulses and tissue absorption from the long time decay of the broadened scattered laser pulses profile (Delpy *et al* 1988, Chance 1998, Alfano *et al* 1997, 1998). Frequency-domain instruments, using radio-frequency-modulated light sources and phase-sensitive detection of the modulated light (which is directly related to the pathlength), enable quantification of tissue absorption and scattering (Fantini *et al* 1994, 1999, Chance 1998). Both time- and frequency-domain methods enable quantification of tissue absorption and scattering, they thus provide absolute determination of haemoglobin concentration.

2.2. Continuous-wave instruments

A continuous-wave (CW) spectrometer consists of two excitation sources and a dual-channel phase-sensitive detection system. A block diagram of the device is shown in figure 1. The excitation source consists of two diode lasers operating at 830 nm and 780 nm. The operating wavelengths straddle the isosbestic point of oxyhaemoglobin (HbO_2) and deoxyhaemoglobin

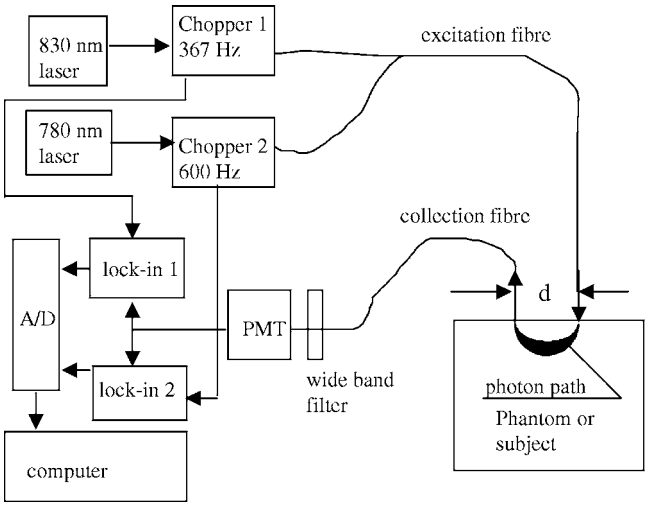

Figure 1. Block diagram of the continuous-wave optical device.

(Hb) absorption near 800 nm. The output of the 830 nm and 780 nm lasers are given low-frequency modulations at 367 Hz and 600 Hz respectively. The excitation light is combined into a single-excitation 1.0 mm optical fibre for delivery to the sample surface. The total power delivered to the subject is 0.25 mW (0.1 mW at 780 nm and 0.15 mW at 830 nm). The output power of the fibre has been set below 0.32 mW for each wavelength.

The scattered light is collected by a 5 mm diameter fibre-optic wave-guide positioned 3 cm from the excitation fibre. A wide-band filter centred at 800 nm removes environmental light noise. Both wavelengths are transmitted by the fibre to a single photomultiplier tube (PMT, model R943 Hamamatsu Inc., Bridgewater, NJ). The output of the PMT is split into two signals, amplified and directed to two lock-in amplifiers (LIA) (Ithaca model 3981, Ithaca Inc., Ithaca, NY) mounted in a personnel computer. Each LIA were tuned to detect one of the low-frequency modulations imparted to the two laser sources. The modulation frequencies were chosen to be well separated from each other and from their respective harmonics. In this configuration, each LIA isolates, amplifies and digitizes the signal from only one laser. The digitized output of the two LIAs is transferred to the computer for storage and further data processing.

The maximum sampling rate of the instrument is 256 Hz for both channels. In this experiment, data were averaged for 1 s improve the signal to noise level. Under these conditions, the noise standard deviation is better than 0.002 OD at both wavelengths, and the output drift is less than 0.004 OD for both optical channels. The cross-talk between two channels is less than 0.5%.

The optical fibre probes were positioned perpendicular to the scalp surface. The source–detector line was centred on the left-hand side of the piglet's head, 1.5 cm from the midline (see figure 2(*a*)). The collection fibre for the CW probe was fixed by a metal plate 0.6 cm from the head. This distance provided visualization of the optical coupling between the fibres and the head. Guide holes in the plate held the excitation fibre in contact with the scalp. In this fashion, good optical contact was achieved on the skin, while the fibres were prevented from retracting from the piglet's head. This maintained the flexibility necessary to adapt the optical probe to the curved surface of the piglet's head.

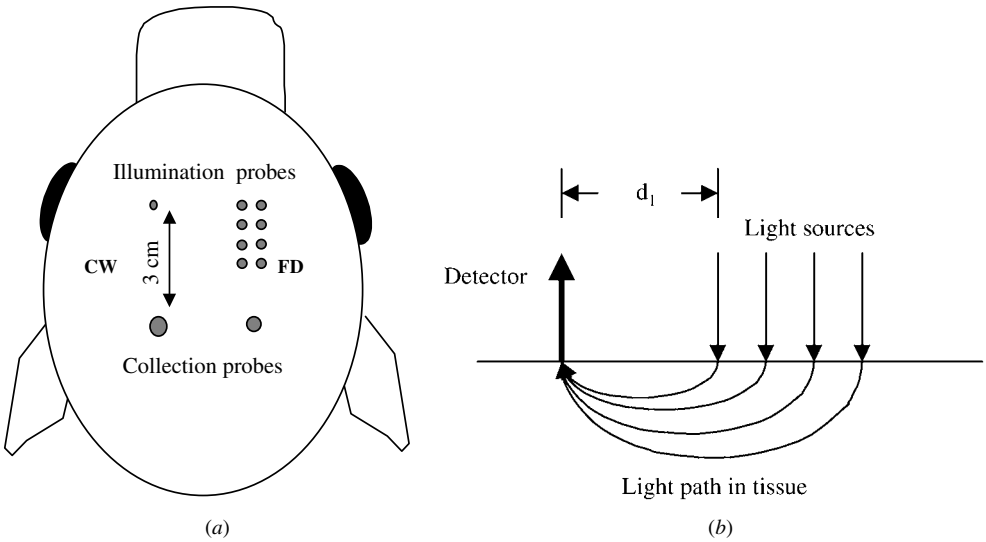

Figure 2. Experimental set-up. (*a*) Schematics of the two (CW and FD) optical probes that were applied to the scalp using the manipulator arm of the stereotactic instrument. (*b*) Schematics of the frequency-domain optical probe geometry with only four source fibres shown.

2.3. CW data processing

In a highly scattering medium such as tissue, the photons travel a mean distance, which is far greater than the geometrical pathlength d (Wyatt 1997, Wahr *et al* 1996, Delpy and Cope 1997, Cope and Delpy 1988, Cope *et al* 1991, Wyatt *et al* 1990). In continuous-wave spectroscopy, changes in tissue chromophore concentrations from the baseline value can be obtained from the modified Beer–Lambert relationship, if the mean optical pathlength is known or can be estimated (Wyatt 1997, Delpy *et al* 1988, Wray *et al* 1988). The Beer–Lambert relationship was modified to include the differential pathlength factor (DPF) B and additive term G due to scattering loss and a multiplier to account for the increased optical pathlength from the scattering:

$$A = \lg(I_0/I) + \alpha c d B + G \tag{1}$$

where A is attenuation measured in OD, I_0 is the light intensity incident on the medium, I is the light intensity transmitted through the medium, α is specific extinction coefficient of the absorbing compound measured in μmol^{-1} cm^{-1}, c is the concentration of the absorbing compound in the medium measured in μmol and d is distance between the points where the light enters and leaves the medium measured in cm (Wyatt 1997, Delpy *et al* 1988, Wray *et al* 1988).

The modified Beer–Lambert law will not yield an absolute measurement of concentration since the G is unknown and dependent upon the measurement geometry and the scattering coefficient of the interrogated tissue. Without knowledge of G, the equation cannot be solved to provide a measure of the absolute concentration of chromophore in medium from a measure of absolute attenuation. If G does not change during the measurement period, it is possible to determine the changes (Δc) in concentration of the chromophore from the measured changes (ΔA) in attenuation as follows:

$$\Delta A = \Delta c \alpha d B. \tag{2}$$

The quantification of the change in concentration still depends on the measurement of the distance d and the differential pathlength factor B, which is the true optical pathlength travelled by the scattered light. For a non-scattering medium the total optical pathlength is equivalent to the straight-line distance d, since the DPF is unity (Wyatt 1997, Wahr *et al* 1996, Delpy and Cope 1997, Cope and Delpy 1988, Cope *et al* 1991, Wyatt *et al* 1990). The differential pathlength factor B was obtained from the FD device, and for piglet head is approximately 6 (Fantini *et al* 1999). For example, for a probe distance of 3 cm, the mean distance of light travel in the head is approximately 18 cm. Since the absolute concentration of chromophore is unknown, all measurements are expected as absolute concentration changes from an arbitrary zero at the start of the measurement period.

2.4. Frequency-domain instrument

A dual-channel frequency-domain tissue spectrometer (model 96208, ISS, Inc., Champaign, IL) allows for the determination of average value (d.c.), amplitude (a.c.), and phase (Φ) of the modulated optical signal intensity at four different source–detector distances at each wavelength. This multidistance method affords the quantitative assessment of the absorption (μ_a) and reduced scattering (μ_s') coefficients of tissues by use of either the (d.c., Φ) or (a.c., Φ) pair of data. In this study, the (a.c., Φ) pair method was used to minimize the effect of possible leakage of room light into the optical probe, and from optical cross-talk with the other CW spectrometer. The eight 400 μm source optical fibres (four guiding light at 758 nm, four at 830 nm), and the 3 mm diameter detector fibre bundle were positioned on the right-hand side of the piglet's head, as shown in figure 2(*a*). The eight laser diodes were multiplexed at a rate of 50 Hz, so that only one light source was on for 20 ms at a time. The average power of the illuminations at the optical fibre probe terminal are about 0.25 mW for 758 nm and about 0.5 mW for 830 nm. The acquisition time per cycle over the eight light sources was 160 ms. An average of 16 cycles was used to get an overall acquisition time of 2.56 s. This was considered to be sufficient to monitor the relatively slow dynamic processes resulting from changes in cerebral haemodynamics and oxygenation. There was no cross-talk detected between these signals from two instruments taking data simultaneously, since the ISS instruments worked with very different modulation frequencies and decoded the signal with lock-in amplifiers at a modulation reference frequency.

The optical probe consisted of eight emitter fibres and one detector fibre-optic bundle arranged at four different source–detector distances ranging from 1.48 to 2.98 cm (figure 2(*a*)). The estimated sampling volume of this probe falls between the minimum of 1.5 cm^3 (1.5 cm length, 1 cm depth, 1 cm width) and the maximum of 12 cm^3 (3 cm length, 2 cm depth, 2 cm width). A medium value of 5 cm^3 (2.5 cm length, 1 cm depth, 2 cm width) would be the most realistic sampling volume of the probe (Stankovic *et al* 2000). One light source is then turned on and light passes from one emitter fibre, through the tissue and into the collector. After the termination of the measurement, the next light source is turned on, and so on. A measurement cycle is complete when all eight light sources have been sequentially turned on and measured.

2.5. FD data processing

In order to make an accurate determination of the absorption coefficient, the scattering coefficient is measured directly. It is able to determine haemoglobin concentration in a high-scattering medium (Fantini *et al* 1994, 1999, Franceschini *et al* 1998, Gratton *et al* 1997). The ISS oximeter determines the μ_a and μ_s' of the tissue by measuring the a.c., d.c. and phase change as function of distance d through the tissue (Fantini *et al* 1994, 1999, Franceschini *et al*

1998, Gratton *et al* 1997). Assuming the geometry presented in figure 2(*b*), and $\mu_s' \gg \mu_a$, light transport through the tissue could be described as following (Fantini *et al* 1994, 1999, Franceschini *et al* 1998, Gratton *et al* 1997):

$$\ln(d^2\,\text{d.c.}) = dS(\text{d.c.}) + K(\text{d.c.}) \tag{3}$$

$$\ln(d^2\,\text{a.c.}) = dS(\text{a.c.}) + K(\text{a.c.}) \tag{4}$$

$$\Phi = dS(\Phi) + K(\Phi) \tag{5}$$

where K are constant and S(a.c.), S(d.c.) and $S(\Phi)$ are slopes of the a.c., d.c. and phase respectively, and d is the distance. The slopes are functions of μ_a and μ_s' and other known parameters such as frequency and speed of light in tissue. After the slopes have been obtained, μ_a and μ_s could be calculated using any two of the slopes, a.c. and phase, or a.c. and d.c., d.c. and phase. For the a.c. and phase pair, μ_a and μ_s' of a semi-infinite medium in the diffusion approximation are given by (Fantini *et al* 1994, 1999, Franceschini *et al* 1998, Gratton *et al* 1997)

$$\mu_a = (\omega/2v)[S(\Phi)/S(\text{a.c.}) - S(\text{a.c.})/S(\Phi)] \tag{6}$$

$$\mu_s' = [S(\text{a.c.})^2 - S(\Phi)^2]/3\mu_a - \mu_a \tag{7}$$

where ω is the angular modulation frequency of the source intensity and v is the speed of light in the tissue. We have previously noticed that the d.c. slope method differs from the DPF method in two important respects: it does not require the changes in μ_a to be small and it measures the absolute value of μ_a. In addition to this, the d.c. slope method is affected by motion artefacts to a lesser extent than the DPF method. However, the condition $r\sqrt{3\mu_a\mu_s'} \gg 1$ implies that, for typical tissue optical properties $\mu_a \sim 0.1$ cm^{-1} and $\mu_s' \sim 10$ cm^{-1}, the d.c. slope method is more accurate at source–detector distances greater than 1.5–2.0 cm (Fantini *et al* 1999).

2.6. Conversion into haemoglobin parameters

After obtaining the absorption (μ_a) or absorption changes (ΔA) from the measurement instrument at least in two wavelengths, the haemoglobin concentration (change) could be calculated by following formula:

$$\text{HbO}_2 = \frac{\mu_a(\lambda_1)E_{\text{Hb}}(\lambda_2) - \mu_a(\lambda_2)E_{\text{Hb}}(\lambda_1)}{E_{\text{HbO}_2}(\lambda_1)E_{\text{Hb}}(\lambda_2) - E_{\text{HbO}_2}(\lambda_2)E_{\text{Hb}}(\lambda_1)} \tag{8}$$

$$\text{Hb} = \frac{\mu_a(\lambda_2)E_{\text{HbO}_2}(\lambda_1) - \mu_a(\lambda_1)E_{\text{HbO}_2}(\lambda_2)}{E_{\text{HbO}_2}(\lambda_1)E_{\text{Hb}}(\lambda_2) - E_{\text{HbO}_2}(\lambda_2)E_{\text{Hb}}(\lambda_1)} \tag{9}$$

for absolute measurement with the FD method instrument, and

$$\Delta\text{HbO}_2 = \frac{\Delta A(\lambda_1)E_{\text{Hb}}(\lambda_2) - \Delta A(\lambda_2)E_{\text{Hb}}(\lambda_1)}{E_{\text{HbO}_2}(\lambda_1)E_{\text{Hb}}(\lambda_2) - E_{\text{HbO}_2}(\lambda_2)E_{\text{Hb}}(\lambda_1)} \tag{10}$$

$$\Delta\text{Hb} = \frac{\Delta A(\lambda_2)E_{\text{HbO}_2}(\lambda_1) - \Delta A(\lambda_1)E_{\text{HbO}_2}(\lambda_2)}{E_{\text{HbO}_2}(\lambda_1)E_{\text{Hb}}(\lambda_2) - E_{\text{HbO}_2}(\lambda_2)E_{\text{Hb}}(\lambda_1)} \tag{11}$$

for relative change measurement with the CW method instrument, where $E_{\text{HbO}_2}(\lambda)$ and $E_{\text{Hb}}(\lambda)$ are known, and indicate the molar extinction coefficient to base e at wavelength λ for complete oxyhaemoglobin and deoxyhaemoglobin molecules.

2.7. Statistical analysis

The goal of comparison studies is to determine whether the two methods agree sufficiently to be used interchangeably. In our study, the correlation analysis was used to assess the strength of

agreement between the CW and FD measurements. The correlation coefficient (r) defines both the strength and the direction of the linear relationship between the measurements obtained by the two methods. However, simple correlation between CW and FD does not disclose whether the difference between the measurements is related to the magnitude of the measurement and, therefore, can be fundamentally misleading (Mantha *et al* 2000).

The Bland and Altman analysis that we used determines whether the difference between the two methods is related to the magnitude of the measurement. The first step was to calculate the difference between the CW and FD measurements (d.c. data) at 758/780 and 830 nm for each animal. The mean of the differences for all six animals (second step) represents the estimated bias (difference between the methods, the measurement of error). The standard deviation (SD) of these differences measures random fluctuations around the mean. If the 'limits of agreement' (mean difference $\pm$ 2SD) between the two methods are not clinically important then the methods can be used interchangeably (Mantha *et al* 2000). The third step was to calculate the average d.c. values for CW and FD at 758/780 and 830 nm for each animal, as well as the average of the means for all six animals. The average of the two methods represents the assumed true value (Mantha *et al* 2000).

The essential feature of the analysis is the graphical representation of the data with CW–FD difference (y-axis) plotted against the CW–FD average (x-axis) (see figure 7). The plot shows the relationship between the measurement of error (difference) and the assumed true value (average). The confidence intervals (CI) for the mean bias $\pm$ 2SD at 758/780 and 830 nm show the extent to which the results can be generalized based on the observed data (Bland and Altman 1995, Mantha *et al* 2000).

2.8. Animal model

This animal study was approved by the Institutional Review Board (IRB) at the Winthrop University Hospital, State University of New York at Stony Brook, Mineola, NY. The animals were treated in accordance with the Guide for the Care and Use of Laboratory Animals by the Institute of Laboratory Animal Resources, National Research Council†. The animal model used for this study has been previously described in the literature (Fantini *et al* 1999, Stankovic *et al* 1999). Briefly, a total of six 9.3 ± 1.9-day-old newborn piglets of either sex, weighing 2.45 ± 1.09 kg were sedated with intramuscular ketamine 20 mg kg^{-1} mixed with xylazine 4 mg kg^{-1}, intubated, and ventilated with an infant ventilator (Bear Medical Systems Inc., Riverside, CA). General anaesthesia was maintained by a continuous intravenous infusion of propofol at a concentration of 0.8 mg ml^{-1} at 4–8 mg kg^{-1} h^{-1}. Both abdominal aorta and inferior vena cava were catheterized to provide direct monitoring of the arterial blood pressure (Hewlett Packard 78353B, USA) and gases (Ciba—Corning 238 pH—blood gas analyzer, Medfield, MA) and intravenous D5W/propofol infusion respectively. Heart rate and arterial oxygen saturation were monitored by pulse oximetry (Nellcor, Hayward, CA) with the probe attached to the pig's tail. The core temperature was maintained at 37 °C with the use of a heating blanket and continuously monitored by a rectal thermometer. To eliminate motion artefacts, the preshaved animal's head was secured within a stereotactic instrument (Lab Standard 51600, Stoelting, Wood Dale, IL) with two 18° ear bars and a nose clamp. The manipulator arm of the stereotactic instrument allowed for three-dimensional positioning of the CW and FD optical probes and optimal probe-to-scalp contact. The CW and FD optical fibres were positioned perpendicularly to the right and left scalp surface respectively. No resuscitation was required at any time. At the end of the study, all piglets were sacrificed by an overdose of sodium pentobarbital (500 mg intravenous injection).

† *NIH Guide*, volume 25, no 28, 16 August, 1996.

Table 1. Physiological data obtained from six newborn piglets (mean ± SD).

Physiological data	Baseline	Max. hyperventilation	Max. hypoventilation
HR (beats/min)	123.8 ± 15.4	127.7 ± 20.9	111.3 ± 14.9
MAP (mm Hg)	72 ± 10.4	55 ± 9.8	54.3 ± 11.5
$PaCO_2$ (mm Hg)	42.2 ± 2.6	13.3±3.3	56.7 ± 5.8
PaO_2 (mm Hg)	119.8 ± 23.9	126.7 ± 27.9	98.7 ± 20.5
pH	7.4 ± 0.07	7.65 ± 0.09	7.16 ± 0.02
SaO_2 (%)	98.02 ± 0.75	99.05 ± 0.28	94.8 ± 2.8

HR, heart rate; MAP, mean arterial pressure; $PaCO_2$, arterial carbon dioxide tension; PaO_2, arterial oxygen tension; SaO_2, arterial oxygen saturation.

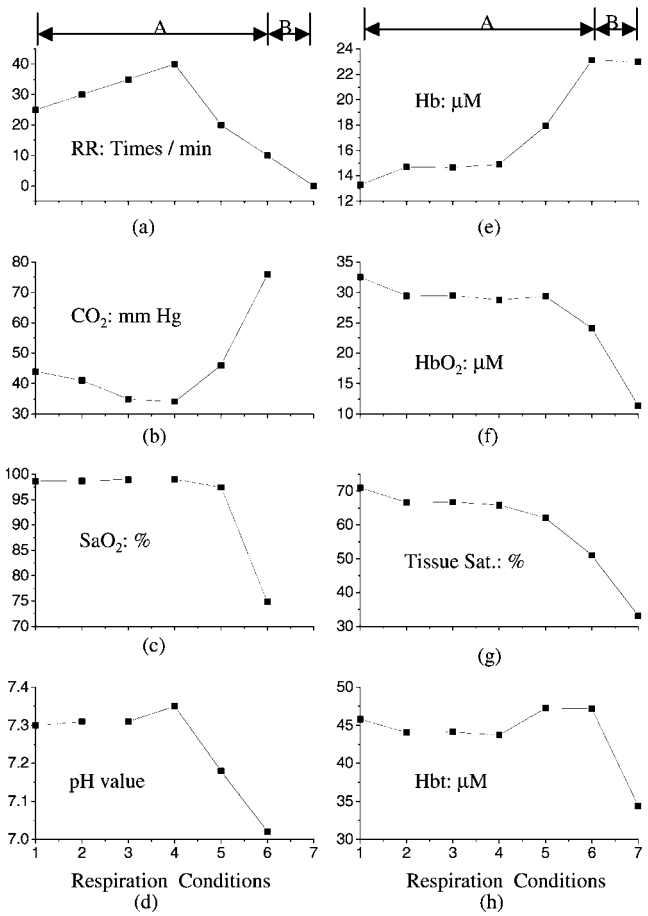

Figure 3. Typical hyper- and hypoventilation-induced changes in conventional variables: (*a*) respiration rate (RR), (*b*) arterial CO_2, (*c*) arterial oxygen saturation (SaO_2), (*d*) pH and cerebral optical variables, (*e*) deoxyhaemoglobin (Hb), (*f*) oxyhaemoglobin (HbO_2), (*g*) total haemoglobin (Hbt) and (*h*) tissue saturation.

2.9. Experimental protocol

After a period of stabilization for piglet, the ventilation was adjusted to ensure the normal values of the arterial blood gasses (figure 3, field 1). Then the baseline optical (d.c., a.c., Φ, μ_a, μ_s', HbO_2, Hb and Hbt (total haemoglobin)) and conventional variables, meaning mean

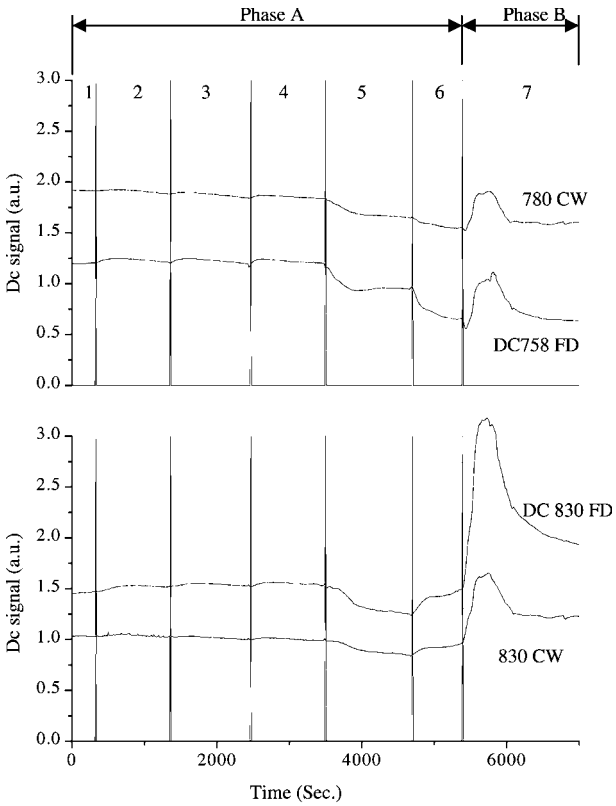

Figure 4. Raw data (d.c. outputs), as recorded by the CW oximeter at 780 and 830 nm with a source–detector separation of 3 cm, and the FD oximeter at 758 and 830 nm with a source–detector separation of 2.98 cm.

arterial blood pressure (mm Hg), heart rate (beats per minute), arterial blood gases (PaO_2 and $PaCO_2$, in mm Hg), pH and arterial oxygen saturation (SaO_2), were recorded. CO_2 is a potent vasodilator. In contrary, every decrease in $PaCO_2$ (hypocarbia) causes vasoconstriction, while a decrease in O_2 (hypoxia), along with an increase in CO_2 (hypercarbia) causes vasodilatation. In our study the arterial pH, O_2 and CO_2 were manipulated by increasing or decreasing the number of respirations per minute, hyper- or hypoventilation respectively. Changes in brain perfusion and oxygenation associated with hyper- and hypoventilation, as detected by the two oximeters, were classified as subtle (figure 3, part A, fields 1–6), as opposed to the large changes accompanying lethal injection of sodium pentobarbital (figure 3, part B, field 7). Lethal sodium pentobarbital injection causes cardiac arrest, cessation of cerebral blood flow and terminal brain asphyxia, followed by cell death as a consequence of hypoxia. As we have previously reported, terminal brain asphyxia is a valuable source of optical information (Fantini *et al* 1999).

3. Results

Table 1 summarizes the systemic physiological data obtained from six animals. All the systemic changes were accompanied by the changes in brain haemodynamics and oxygenation, as detected by both CW and FD optical instruments. As for the optically detected brain

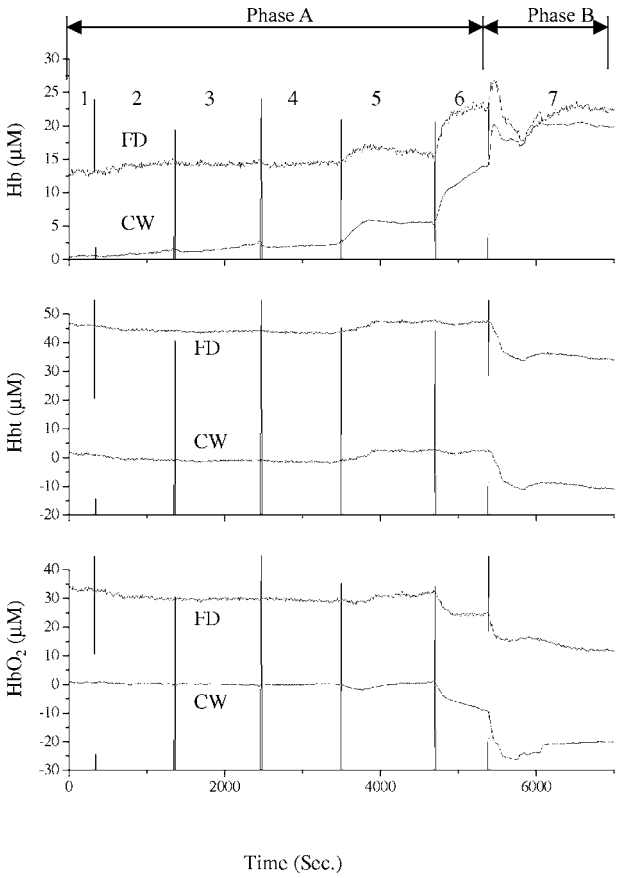

Figure 5. Haemoglobin parameters (i.e. Hb, HbO_2 and Hbt) recorded by the CW oximeter at 780 and 830 nm, and the FD oximeter at 758 and 830.

perfusion–oxygenation changes, all animals responded to the ventilation changes and the cardiac arrest with a great deal of reproducibility (table 2, figures 3–6). Optical tracings were divided into two segments, phase A and phase B, according to the magnitude of changes (subtle changes, phase A; large changes, phase B). Figure 3 illustrates typical systemic and optical changes (FD instrument) recorded in one animal.

Figure 4 compares the raw (d.c.) data recorded by the CW instrument at 780 and 830 nm with a source–detector separation of 3 cm, and the FD instrument at 758 and 830 nm with a source–detector separation of 2.98 cm. Figure 5 compares the processed data (Hb, HbO_2 and Hbt) recorded by the CW instrument (at 780 and 830 nm, source–detector separation 3 cm) and the FD instrument (at 758 and 830 nm, the multidistance approach).

Hyperventilation (an increase in the respiratory rate) caused a decrease in $PaCO_2$, mean arterial blood pressure (MAP) and heart rate (HR), as well as an increase in pH, without affecting PaO_2 and SaO_2 (table 1, figure 3). In the brain, hyperventilation caused positive changes in d.c. at 758/780 nm, negative changes at 830 nm (figure 4, fields 1, 2 and 3), and consecutively increase in Hb, and decrease in HbO_2, Hbt and tissue saturation (figure 3, figure 5, fields 1, 2 and 3).

Hypoventilation (a decrease in the respiratory rate), on the other hand, caused an increase in $PaCO_2$, and decrease in HR, MAP, PaO_2, pH and SaO_2 (table 1, figure 3). In the brain,

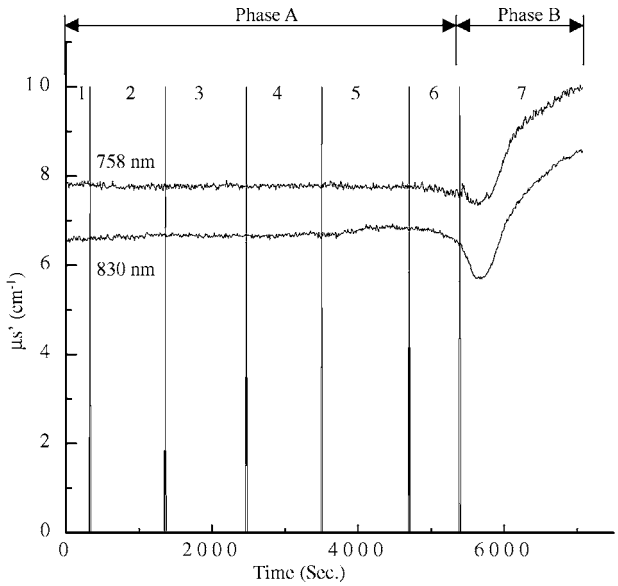

Figure 6. Brain tissue scattering changes detected by the FD oximeter.

Table 2. Correlation between the frequency-domain (FD) and continuous-wave (CW) oximeters. In phase A is the subject still alive with different ventilation conditions; phase B is the dying subject after sacrifice by injection of an over-dose of pentobarbital.

1	2	3	4		5		6	
Piglet no	FD @ 758 nm versus CW @ 780 nm	FD @ 830 nm versus CW @ 830 nm	Hb		HbO_2		Hbt	
			Phase A	Phase B	Phase A	Phase B	Phase A	Phase B
1	0.96	0.99	0.89	0.57	0.91	0.49	0.95	0.48
2	0.95	0.98	0.97	0.28	0.87	0.01	0.85	0.31
3	0.92	0.96	0.95	0.86	0.92	0.85	0.93	0.87
4	0.93	0.98	0.85	0.65	0.96	0.41	0.98	0.16
5	0.98	0.91	0.98	0.58	0.9	0.46	0.87	0.67
6	0.91	0.97	0.95	0.51	0.95	0.45	0.94	0.42

hypoventilation caused negative changes in d.c. at 758/780 nm, positive changes at 830 nm (figure 4, fields 4 and 5), and consecutively increase in Hb and Hbt, and decrease in HbO_2 and tissue saturation (figure 3, figure 5, fields 4 and 5).

Cardiac arrest and apnoea caused a further increase in $PaCO_2$, as well as a decrease in HR, MAP, pH, O_2 and SaO_2 (figure 3). In the brain, cardiac arrest and apnoea caused further negative changes in d.c. at 758/780 nm, positive changes at 830 nm (figure 4, fields 6 and 7), and consecutively increase in Hb and Hbt, and decrease in HbO_2, Hbt and tissue saturation (figure 3, figure 5, fields 6 and 7).

Table 2 shows the correlations between the raw (d.c.) CW and FD data (table 2, columns 2 and 3) and the processed CW and FD data (table 2, columns 4, 5, 6). For the raw data, an excellent correlation between the CW and FD instruments was noted at all wavelengths. For the processed data, an excellent correlation was noted only during the phase A (in all six animals).

Scattering changes (ISS FD oximeter) were associated only with asphyxia and death (figure 6, fields 6 and 7).

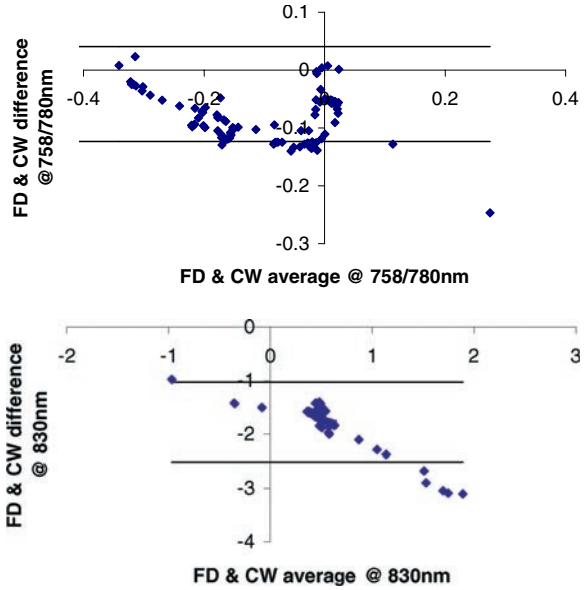

Figure 7. Average against difference of the test (CW) and standard (FD) measurements, with 95% limits of agreement (lines) at 758/780 nm and 830 nm for all six animals.

In order to show how far apart the CW and FD were likely to be (the recommended 95% limits of agreement) we used mean difference ± 2SDs (Bland and Altman 1995). Figure 7 shows the plot of the average against the difference between the test (CW) and standard (FD) measurements, with 95% limits of agreement (broken lines) at 758/780 nm and 830 nm for six piglets. For the 758/780 nm data, the correlation between the difference and average was −0.29 (95% CI −0.12 to 0.04, $p = 0.02$). For the 830 nm data, the correlation between the difference and average was −0.88 (95% CI −2.52 to −1.04, $p = 0.02$). A trend in the bias, i.e. a tendency for the mean difference to fall with increasing magnitude of the detected optical changes (and consecutively FD–CW difference), shows that the methods did not agree equally through the range.

4. Discussion

The brain is critically dependent on oxygenation for function and viability. The critical point in the prevention of neonatal brain injury would be the maintenance of cerebral perfusion through prevention of severe hypotension and avoidance of marked cerebral vasoconstriction that can be induced by hypocarbia (Volpe 1997) (figures 3–6). This and several other studies have shown that optical spectroscopy can play a critical role in the recognition and detection of disturbances in cerebral haemodynamics and oxygenation associated with changes in blood oxygenation and CO_2 (Pryds *et al* 1990, Pollard *et al* 1996b, Wyatt *et al* 1991, Stankovic *et al* 1998b, Fantini *et al* 1999).

Although spectroscopy of blood can be traced back to the 1870s (Chance *et al* 1997), the first attempt to measure tissue perfusion in normoxia and ischaemia took place in the 1930s, when the first filter wheel apparatus for finger spectroscopy was developed (Chance *et al* 1997), followed by Kramer's single-beam apparatus using a Siemens barrier layer (1935), Millikan's dual-wavelength haemoglobinometer (1936), and Matthes and Gross' ear oximeter

(1939) (Chance *et al* 1997). It was in 1977 that Jobsis first described the *in vivo* application of near-infrared spectroscopy to monitor changes in the oxygenation of the brain in the intact cat head (Jobsis 1977). Since 1977, tremendous research and development has taken place, leading to several experimental and/or commercial instruments, continuous-wave (Alfano *et al* 1998, Chance 1998, Cope and Delpy 1988, Pollard *et al* 1996a, Jobsis 1977), time-domain (Benaron *et al* 1992, Delpy *et al* 1988, Chance 1998), and frequency-domain (Chance 1998, Chance *et al* 1998, Gratton *et al* 1997).

Continuous-wave spectroscopy is based on several assumptions.

(a) That HbO and Hb are the dominant tissue chromophores.
(b) That the background attenuation does not change during the course of experiment.
(c) That tissue is optically homogeneous with no regional variations in absorption or scattering.
(d) That the spatial distribution of HbO_2 and Hb will remain constant during the experiment.
(e) That there is a negligible contribution from the extracerebral haemoglobin (scalp and skull) to the near-infrared spectroscopy signal.
(f) That the physical geometry of the optical probe will remain constant.
(g) That tissue scattering characteristics are known and will remain constant throughout the experiment (Wyatt 1997).

It is clear that deviations from these assumptions are likely to lead to significant error (Wyatt 1997).

Over the past several years significant validation efforts have been made. Optical spectroscopy has been validated with sagittal sinus (Ferrari *et al* 1989) and jugular vein blood sampling (Cruz and Miner 1986, Pollard *et al* 1996b), ^{133}Xe clearance (Pryds *et al* 1990, Skov *et al* 1991, Goddard-Finegold *et al* 1998), vascular Doppler techniques (Stankovic *et al* 1998a, b, Hintz *et al* 1999), radioactive-labelled microspheres (Tsuji *et al* 1998, Goddard-Finegold *et al* 1998), computer tomography (Hintz *et al* 1999), magnetic resonance spectroscopy (Tsuji *et al* 1995) and imaging (Hintz *et al* 1999). Still, the single high-priority goal defined by the 1992 NIH-NINDS Workshop on Near Infrared Spectroscopy that '. . . data should be comparable between different NIRS instruments and methods . . .' (Hirtz 1993) has not been sufficiently addressed so far. However, this study is, to our knowledge, one the very few to correlate CW and FD methods. Ferrari *et al* (1995) have demonstrated the agreement between the measurements in the muscle (ischaemia) and the brain (postural changes) obtained with the FD (first generation ISS spectrometer, i.e. OMNIA, ISS, Champaign, IL) and the CW instrument (NIRO 500, Hamamatsu Photonics, Japan). Grubhofer *et al* (1999) compared two continuous-wave oximeters, namely INVOS 3100 and NIRO 500, during and after hypocapnia in 15 awake, healthy volunteers, who hyperventilated to obtain end-tidal CO_2 values of approximately 20 mm Hg. The authors correlated their optical results with end-tidal CO_2 values. They found that cerebral haemoglobin oxygenation states were reflected more accurately by INVOS 3100 than by NIRO 500. They speculated that the cause may be the different technology of the monitors, since INVOS 3100 eliminates the contribution of extracranial oxygenation (Grubhofer *et al* 1999).

Our results have shown an excellent correlation between the two d.c. signals at 758 (FD), 780 (CW) and 830 (FD and CW) (table 2, columns 2 and 3; figure 4). The correlation between the processed data (haemoglobin changes) was high only during the events associated with no change in μ_s (figure 6) and subtle changes in μ_a (table 2, columns 4, 5 and 6). The differences could be attributed to the differences in sampling volumes of the CW and FD probes as well as the structural differences between the left and the right hemisphere of the brain (Delpy and Cope 1997, Stankovic *et al* 2000). Poor correlation between the processed

CW and FD measurements (haemoglobin data) associated with the large changes in absorption and scattering (death) are probably related to the inability of the CW system to determine μ_a and μ_s. Therefore, absolute determination of the optical properties of tissue is critical. One should not forget that all the approaches are limited by the accuracy of the models of light transport in inhomogeneous media (Delpy and Cope 1997).

5. Conclusion

This study describes the correlation between the signals obtained simultaneously with two different optical instruments, continuous-wave and frequency-domain, in a newborn piglet brain perfusion–oxygenation model. The results have shown that continuous-wave spectroscopy, although incapable of absolute determination of the optical properties of tissue, was able to detect and monitor both small and large changes in brain haemodynamics and oxygenation. This is in agreement with Chance's remark that despite the advantages of time-domain in FD methods, much information can be obtained with the pathlength-scrambled d.c. signals obtained with continuous light (Chance *et al* 1997).

Acknowledgments

We cordially thank Dennis Huber and Don Wallace of ISS Inc. for their technical assistance with the ISS Oximeter and their review of commentary on this paper. We also thank Jean Handel, Darrin Chester, Pauline Bitteto and Patricia Johnson for their technical assistance. This work has been supported by the DOE Center of Excellence Program.

References

Alfano R R, Demos S G and Gayenr S K 1997 Advances in optical imaging of biomedical media *Ann. NY Acad. Sci.* **820** 248–70

Alfano *et al* 1998 Time-resolved and nonlinear optical imaging for medical applications *Ann. NY Acad. Sci.* **838** 14–28

Benaron D A, Benitz W E, Ariagno R L and Stevenson D K 1992 Noninvasive methods for estimating *in vivo* oxygenation *Clin. Pediatr.* **31** 258–73

Benaron D A, Cheong W F and Stevenson D K 1997 Tissue optics *Science* **276** 2002–3

Bland J M and Altman D G 1995 Comparing methods of measurement: why plotting difference against standard method is misleading *Lancet* **346** 1085–7

Brazy J E 1991 Cerebral oxygen monitoring with near infrared spectroscopy: clinical application to neonates *J. Clin. Monit.* **7** 325–34

Brun N C, Moen A, Borch K, Saugstad O D and Greisen G 1997 Near-infrared monitoring of cerebral tissue oxygen saturation and blood volume in newborn piglets *Am. J. Physiol.* **273** H682–6

Chance B 1998 Near-infrared images using continuous, phase-modulated, and pulsed light with quantitation of blood and blood oxygenation *Ann. NY Acad. Sci.* **838** 29–45

Chance B, Cope M, Gratton E, Ramanujam N and Tromberg B 1998 Phase measurement of light absorption and scatter in human tissue *Rev. Sci. Instrum.* **69** 3457–81

Chance B, Luo Q, Nioka S, Alsop D C and Detre J A 1997 Optical investigations of physiology: a study of intrinsic and extrinsic biomedical contrast *Phil. Trans. R. Soc.* B **352** 707–16

Cope M and Delpy D T 1988 System for long-term measurement of cerebral blood flow and tissue oxygenation on newborn infants by infra-red transillumination *Med. Biol. Eng. Comput.* **26** 289–94

Cope M, Van Der Zee P, Essenpreis M E, Arridge S R and Delpy D T 1991 Data analysis methods for near infrared spectroscopy of tissues: problems in determining the relative cytochrome aa3 concentration *Proc. SPIE* **1431** 251–62

Cruz J and Miner M E 1986 Modulating cerebral oxygen delivery and extraction in acute traumatic coma *Neurotrauma* ed W Ka (Boston: Butterworth) pp 55–72

Delpy D T and Cope M 1997 Quantification in tissue near-infrared spectroscopy *Phil. Trans. R. Soc.* B **352** 649–59

Delpy D T, Cope M, van der Zee P, Arridge S, Wray S and Wyatt J 1988 Estimation of optical pathlength through tissue from direct time of flight measurement *Phys. Med. Biol.* **33** 1433–42

Fantini S, Franceschini M A and Gratton E 1994 Semi-infinite-geometry boundary problem for light migration in highly scattering media: a frequency-domain study in the diffusion approximation *J. Opt. Soc. Am.* B **11** 2128–38

Fantini S, Hueber D, Franceschini M A, Gratton E, Rosenfeld W, Stubblefield P G, Maulik D and Stankovic M R 1999 Non-invasive optical monitoring of the newborn piglet brain using continuous wave and frequency domain spectroscopy *Phys. Med. Biol.* **44** 1543–63

Ferrari M, De Blasi R A, Fantini S, Franceschini M A, Barbieri B, Quaresima V and Gratton E 1995 Cerebral and muscle oxygen saturation measurement by a frequency-domain near-infrared spectroscopic technique *Proc. SPIE* **2389** 868–74

Ferrari M *et al* 1989 Determination of cerebral venous haemoglobin saturation by derivative near infrared spectroscopy *Adv. Exp. Med. Biol.* **248** 47–53

Franceschini M A, Fantini S, Paunescu L A, Maier J S and Gratton E 1998 Influence of a superficial layer in the quantitative spectroscopic study of strongly scattering media *Appl. Opt.* **37** 7447–58

Goddard-Finegold J, Louis P T, Rodriguez D L, David Y, Contant C F and Rolfe P 1998 Correlation of near infrared spectroscopy cerebral blood flow estimations and microsphere quantitations in newborn piglets *Biol. Neonate* **74** 376–84

Gratton E, Fantini S, Franceschini M A, Gratton G and Fabiani M 1997 Measurements of scattering and absorption changes in muscle and brain *Phil. Trans. R. Soc.* B **352** 727–35

Grubhofer G, Tonninger W, Keznickl P, Skyllouriotis P, Ehrlich M, Hiesmayr M and Lassnigg A 1999 A comparison of the monitors INVOS 3100 and NIRO 500 in detecting changes in cerebral oxygenation *Acta Anaesthesiol. Scand.* **43** 470–5

Hintz S R, Cheong W F, van Houten J P, Stevenson D K and Benaron D A 1999 Bedside imaging of intracranial haemorrhage in the neonate using light: comparison with ultrasound, computed tomography, and magnetic resonance imaging *Pediatr. Res.* **45** 54–9

Hirtz D G 1993 Report of the National Institute of Neurological Disorders and Stroke workshop on near infrared spectroscopy *Pediatrics* **91** 414–17

Jobsis F F 1977 Noninvasive infrared monitoring of cerebral and myocardial sufficiency and circulatory parameters *Science* **198** 1264–7

Kurth C D, Steven J M, Benaron D and Chance B 1993 Near-infrared monitoring of cerebral circulation *J. Clin. Monit.* **9** 163–70

Mantha S, Roizen M, Fleisher L A, Thisted R and Foss J 2000 Comparing methods of clinical measurement: reporting standards for Bland and Altman analysis *Anesth. Analg.* **90** 593–602

Meek J H, Tyszczuk L, Elwell C E and Wyatt J S 1998 Cerebral blood flow increases over the first three days of life in extremely preterm neonates *Arch. Dis. Child. Fetal Neonatal Ed.* **78** F33–F37

Nelson K B and Ellenberg J H 1986 Antecedents of cerebral palsy: multivariate analysis of risk *New Engl. J. Med.* **315** 81

Perlman J M, Kreusser K and Volpe J J 1984 The effect of eliminating fluctuating cerebral blood flow velocity in preterm infants with respiratory distress syndrome on the incidence and severity of intraventricular haemorrhage *Ann. Neurol.* **16** 380

Pollard V, Prough D S, DeMelo A E, Deyo D J, Uchida T and Stoddart H F 1996a Validation in volunteers of a near-infrared spectroscope for monitoring brain oxygenation *in vivo Anesth. Analg.* **82** 269–77

Pollard V, Prough D S, DeMelo A E, Deyo D J, Uchida T and Widman R 1996b The influence of carbon dioxide and body position on near infrared spectroscopic assessment of cerebral haemoglobin oxygen saturation *Anesth. Analg.* **82** 278–7

Pryds O, Greisen G, Skov L L and Friis-Hansen B 1990 Carbon dioxide-related changes in cerebral volume and cerebral blood flow in mechanically ventilated preterm neonates: comparison of near infrared spectrophotometry and ^{133}Xe clearance *Pediatr. Res.* **27** 445–9

Skov L, Pryds O and Greisen G 1991 Estimating cerebral blood flow in newborn infants: comparison of near infrared spectroscopy and ^{133}Xe clearance *Pediatr. Res.* **30** 570–3

Stankovic M R, Fujii A, Maulik D, Boas D, Kirby D and Stubblefield P G 1998c Optical monitoring of cerebral haemodynamics and oxygenation in the neonatal piglet *J. Maternal Fetal Invest.* **8** 71–8

Stankovic M R, Fujii A, Maulik D, Kirby D and Stubblefield P G 1998b Optical brain monitoring of the cerebrovascular effects induced by the acute cocaine exposure in neonatal pigs *J. Maternal Fetal Invest.* **8** 108–12

Stankovic M R, Maulik D, Boas D A and Stubblefield P G 1998a Emerging technologies: fetal optical monitoring *Asphyxia and Fetal Brain Damage* ed M D Coey (New York: Wiley) pp 345–64

Stankovic M R, Maulik D, Rosenfeld W, Stubblefield P G, Kofinas A D, Drexler S, Nair R, Franceschini M A, Hueber D, Gratton E and Fantini S 1999 Real-time optical imaging of experimental brain ischaemia and haemorrhage in neonatal piglets *J. Perinatol.* **27** 1–8

Stankovic M R, Maulik D, Rosenfeld W, Stubblefield P G, Kofinas A D, Gratton E, Franceschini M A, Fantini S

and Hueber D 2000 The role of frequency domain optical spectroscopy in the detection of neonatal brain haemorrhage—a newborn piglet study *J. Maternal Fetal Med.* **9** 142–9

Tsuji M, du Plessis A, Taylor G, Crocker R and Volpe J J 1998 Near infrared spectroscopy detects cerebral ischaemia during hypotension *Pediatr. Res.* **44** 591–5

Tsuji M, Naruse H, Volpe J and Holtzman D 1995 Reduction in cytochrome aa3 measured by near-infrared spectroscopy predicts cerebral energy loss in hypoxic piglets *Pediatr. Res.* **37** 253–9

Van Houten J P, Benaron D A, Spilman S and Stevenson D K 1996 Imaging brain injury using time resolved near infrared light scanning *Pediatr. Res.* **39** 470–6

Volpe J J 1989 Intraventricular haemorrhage and brain injury in the premature infant. Neuropathology and pathogenesis *Clin Perinatol.* **16** 361–86

——1997 Brain injury in the premature infant—from pathogenesis to prevention *Brain Devel.* **19** 519–34

Wahr J A, Tremper K K, Samra S and Delpy D T 1996 Near-infrared spectroscopy: theory and applications *J. Cardiothorac. Vasc. Anesth.* **3** 406–18

Wray S, Cope M and Delpy D T 1988 Characteristics of the near infrared absorption spectra of cytochrome aa3 and haemoglobin for the noninvasive monitoring of cerebral oxygenation *Biochim. Biophys. Acta.* **933** 184–92

Wyatt J S 1997 Cerebral oxygenation and haemodynamics in the foetus and newborn infant *Phil. Trans. R. Soc.* B **352** 697–700

Wyatt J S, Cope M, Delpy D T, Richardson C E, Edwards A D, Wray S and Reynolds E O 1990 Quantification of cerebral blood volume in newborn infants by near infrared spectroscopy *J. Appl. Phys.* **68** 1086–91

Wyatt J S, Edwards A D, Cope M, Delpy D T, McCormick D C, Potter A and Reynolds E O 1991 Response of cerebral blood volume to changes in arterial carbon dioxide tension in preterm and term infants *Pediatr. Res.* **29** 553–7